CHANNELS
2025, VOL. 19, NO. 1, 2473074
https://doi.org/10.1080/19336950.2025.2473074

Taylor & Francis
Taylor & Francis Group

RESEARCH ARTICLE

OPEN ACCESS Check for updates

Role of the C-terminal domain in modifying pH-dependent regulation of $Ca_v1.4$ Ca^{2+} channels

Juan de la Rosa Vázquez and Amy Lee

Department of Neuroscience and Center for Learning and Memory, The University of Texas at Austin, Austin, TX, USA

ABSTRACT

In the retina, Ca^{2+} influx through $Ca_v1.4$ Ca^{2+} channels triggers neurotransmitter release from rod and cone photoreceptors. Changes in extracellular pH modify channel opening, enabling a feedback regulation of photoreceptor output that contributes to the encoding of color and contrast. However, the mechanisms underlying pH-dependent modulation of $Ca_v1.4$ are poorly understood. Here, we investigated the role of the C-terminal domain (CTD) of $Ca_v1.4$ in pH-dependent modulation of Ba^{2+} currents (I_{Ba}) in HEK293T cells transfected with the full length $Ca_v1.4$ (FL) or variants lacking portions of the CTD due to alternative splicing (Δe47) or a disease-causing mutation (K1591X). While extracellular alkalinization caused an increase in I_{Ba} for each variant, the magnitude of this increase was significantly diminished (~40–50%) for both CTD variants; K1591X was unique in showing no pH-dependent increase in maximal conductance. Moreover, the auxiliary $\alpha_2\delta$-4 subunit augmented the pH sensitivity of I_{Ba}, as compared to $\alpha_2\delta$-1 or no $\alpha_2\delta$, for FL and K1591X but not Δe47. We conclude that the CTD and $\alpha_2\delta$-4 are critical determinants of pH-dependent modulation of $Ca_v1.4$ and may influence the processing of visual information in normal and diseased states of the retina.

ARTICLE HISTORY
Received 11 November 2024
Revised 14 February 2025
Accepted 21 February 2025

KEYWORDS
Calcium channel; retina; photoreceptor; pH

Introduction

In the nervous system, changes in the pH of the extracellular environment are linked to aberrant neuronal activity in epilepsy, stroke, and chronic pain [1,2]. Because of the high concentration of protons in synaptic vesicles [3], the fusion of synaptic vesicles with the presynaptic membrane can cause extracellular pH to fall as low as 6.5 [4]. Less severe pH changes occur within the synaptic cleft during normal periods of synaptic activity [5,6]. Because numerous ion channels are modulated by protons [7–9], even minor alterations in the extracellular pH can greatly modify information transfer across synapses.

pH changes have particularly prominent effects on presynaptic Ca_v1 L-type Ca^{2+} channels at ribbon-type synapses in the eye and ear [10–12]. These synapses are characterized by a high rate of glutamate release, which is facilitated by a ribbon organelle that helps prime synaptic vesicles for exocytosis [13]. At retinal and cochlear ribbon synapses, low extracellular pH strongly inhibits the amplitude of presynaptic Ca_v1 currents [10,12,14] and diminishes synaptic output [6,11,15]. At photoreceptor synapses, high extracellular pH shifts the current-voltage (I-V) relationship of presynaptic Ca_v1 channels to more negative voltages [16–18]. Although the underlying mechanisms are controversial, this form of Ca_v1 modulation is thought to be crucial for the mechanisms that encode color and contrast in the retina [10,18,19].

$Ca_v1.4$ is the major Ca_v subtype that mediates neurotransmitter release from rod and cone photoreceptors [20]. In addition to a pore-forming α_{1F} subunit (hereafter referred to as $Ca_v1.4$), these channels contain the auxiliary $\alpha_2\delta$-4 and β_2 subunits [20,21]. Mutations in the *CACNA1F* and *CACNA2D4* genes which encode $Ca_v1.4$ and $\alpha_2\delta$-4, respectively, cause vision disorders including congenital stationary night blindness type 2 (CSNB2) [20]. The *CACNA1F* transcript undergoes extensive alternative splicing

CONTACT Amy Lee amy.lee1@austin.utexas.edu

particularly in the region corresponding to the large cytoplasmic C-terminal domain (CTD, Figure 1) [22,23]. The CTD contains modulatory sequences that inhibit Ca^{2+}-dependent inactivation (CDI) and voltage-dependent activation [22–26]. How these alterations in the CTD might impact physiological forms of $Ca_v1.4$ modulation, such as by extracellular pH, are unknown.

In this study, we aimed to bridge this gap by comparing pH-dependent modulation of the full-length $Ca_v1.4$ ($Ca_v1.4$ FL) and variants lacking portions of the CTD due to alternative splicing ($Ca_v1.4\Delta e47$) or a CSNB2-causing mutation (K1591X). Exon 47 encodes a portion of a C-terminal modulatory domain (CTM) in the CTD (Figure 1). The CTM suppresses CDI in part by competing with calmodulin (CaM) for binding to a consensus IQ domain site in the proximal CTD [24,25]. Deletion of exon 47 does not affect CaM binding, but significantly strengthens CDI while causing a ~10 mV hyperpolarizing shift in the voltage-dependence of activation [23,26]. In K1591X, truncation of the entire CTD downstream of the IQ domain causes a stronger hyperpolarizing shift in activation (~20–30 mV) as well as robust CDI [24,26]. We find that compared to $Ca_v1.4$FL, $Ca_v1.4\Delta e47$ and K1591X show weaker potentiation by extracellular alkalinization. Moreover, omission of $\alpha_2\delta$-4, or its substitution by the $\alpha_2\delta$-1 subtype, significantly alters the extent to which pH changes affect voltage-dependent activation of $Ca_v1.4$FL and K1591X but not $Ca_v1.4\Delta e47$. Our findings add to the modulatory functions of the CTD and raise the possibility that abnormal regulation by pH could contribute to visual impairment caused by pathological variants of *CACNA1F* and *CACNA2D4*.

Materials and methods

HEK293T cell culture and transfection

Human embryonic kidney (HEK) 293T cells, a subclone of the HEK 293 cell line, were acquired from the American Type Cell Culture Collection (ATCC CRL-11268) and maintained in Dulbecco's

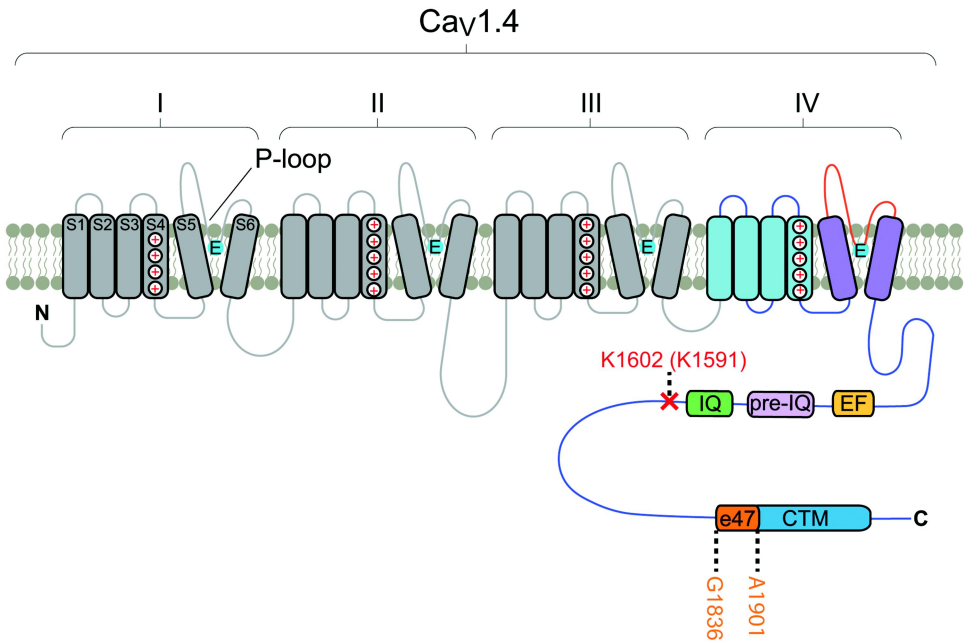

Figure 1. Schematic of $Ca_V1.4$ showing key modulatory regions in the C-terminal domain (CTD). $Ca_v1.4$ (UniProt: O60840) consists of four homologous domains (I-IV), each containing six transmembrane helices (S1-S6, with charged S4) and pore (P) loop containing glutamate (E) residue that contributes to selectivity filter. There is a large C-terminal domain containing an EF-hand domain (EF, L1459-K1478), pre-IQ domain (pre-IQ, N1524-E1568), IQ domain (IQ, V1569-R1597), and a distal C-terminal modulatory domain (CTM) containing exon 47 (e47). X depicts truncation after K1602 (equivalent to (K1591X) due to CSNB2-related mutation. Exon 47 comprises 65 residues, from G1836 to A1901.

modified Eagle's medium with 10% of fetal bovine serum and 1% penicillin/streptomycin, at 37°C in 5% CO_2. The cells were grown to 70–80% confluence and co-transfected with human cDNAs encoding $Ca_V1.4$ FL (GenBank # AF201304), $Ca_V1.4\Delta47$ or K1591X, and $\beta_{2\times13}$ (GenBank #AF465485) and $\alpha_2\delta$-4 (GenBank #NM_172364) or $\alpha_2\delta$-1 (GenBank #NM_000722.4) and pEGFP cDNA for visual identification of transfected cells. The cloning of $Ca_V1.4\Delta47$ and K1591X were described previously [23,26]. FuGENE HD transfection reagent (Promega) was used according to the manufacturer's protocol. After transfection, cells were maintained at 37°C in 5% CO_2 for 24 h and then were dissociated and plated at low density for single cell electrophysiological recordings.

Electrophysiological recordings

Whole-cell patch clamp recordings of the transfected cells were performed 36–72 h after transfection at room temperature. Data were acquired with an EPC-10 USB patch clamp amplifier driven by PatchMaster software (HEKA Elektronik) and analyzed with Igor Pro software (Wavemetrics). Extracellular recording solutions contained (in mM): 140 Tris, 1 $MgCl_2$, and 20 $BaCl_2$. Intracellular solution consisted of (in mM): 140 N-methyl-D-glucamine, 10 HEPES, 2 $MgCl_2$, 2 Mg-ATP, and 5 EGTA. The pH of intracellular and extracellular recording solutions was adjusted to 7.3, or to the indicated value with methanesulfonic acid. The exchange of external solutions (pH 6.25, 6.7, 7.3, 7.5 and 8.0) was performed using a Valve Bank II perfusion system (AutoMate Scientific). Electrode resistances were typically 4–6 MΩ in the bath solution and series resistance compensated up to 70%. Leak subtraction was conducted using a P/4 protocol.

Data analysis

All average data are presented as the mean ± SEM The data were first analyzed for normality using the Shapiro-Wilk test. Statistical significance differences were determined by regression slope test, one-way ANOVA and post hoc Tukey's tests for parametric data or Kruskal-Wallis and post hoc Dunn's tests for non-parametric data, using Prism software (Graph Pad). Normalized current-voltage (I-V) data were fit to the Boltzmann equation (Eq. 1), where G_{max} is the maximal conductance, V_m is the test voltage, V_{rev} represents the apparent reversal potential, V_h is the voltage of half maximal activation, and k is the slope factor.

$$I = G_{max}(V_m - V_{rev})/(1 + \exp[-(V_m - V_h))/k]) \quad \text{(Eq.1)}$$

The IC_{50} for proton block was obtained according to Eq. 2, where f_V is the % of I_{Ba} at pH 8.0, $[H^+]$ is proton concentration in the extracellular solution perfused onto the cell in μM, and α is the Hill slope.

$$f_V = 100/\left(1 + (IC_{50}/[H^+])^{\alpha}\right) \quad \text{(Eq.2)}$$

Results

Extracellular alkalinization hyperpolarizes the voltage-dependence of $Ca_v1.4$ FL activation

The effect of pH on $Ca_v1.4$ was previously studied in channels reconstituted with the β_{2a} and $\alpha_2\delta$-1 subunits [9]. However, $Ca_v1.4$ channels in the retina are thought to contain $\alpha_2\delta$-4 and the $\beta_{2\times13}$ splice variant [21,27]. To gain insights into how pH regulates the native $Ca_v1.4$ complex in photoreceptors, we performed patch clamp recordings of HEK293T cells cotransfected with cDNAs encoding $Ca_v1.4$ FL, $\beta_{2\times13}$, and $\alpha_2\delta$-4. I-V relationships were obtained for Ba^{2+} currents (I_{Ba}) before and after perfusion with extracellular solutions of different pH. The amplitude of I_{Ba} progressively increased as the extracellular pH was raised from 6.25 to 8.0 (Figure 2a). To assess the pH-dependence of this effect, parameters from Boltzmann fits of the I-V data were plotted against pH. Linear regression of these data revealed that alkalinization caused a significant hyperpolarization of the voltage of half-maximal activation (V_h), increase in maximal conductance (G_{max}), and modest decrease in the slope factor (k, Figure 2b–d). In contrast to previous work [9], the reversal potential (V_{rev}) became hyperpolarized with

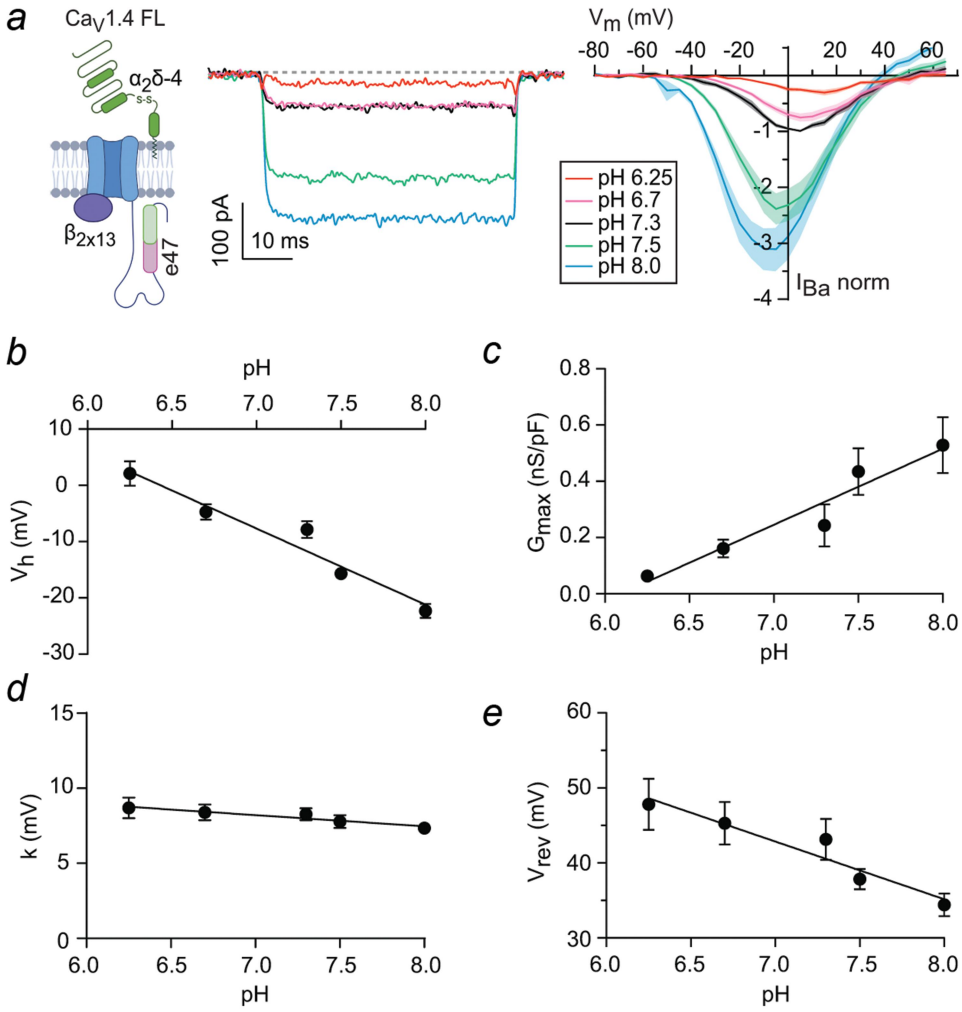

Figure 2. pH-dependent modulation of I_{Ba} in cells transfected with $Ca_V1.4$ FL. (a) Representative traces and I-V plot for I_{Ba} elicited by 50-ms pulses from −80 mV to various voltages. Current traces represent I_{Ba} in a single cell evoked by test pulses evoking the peak I_{Ba} at the indicated pH values (with increasing pH: +10, +5, +5, −5 and −10 mV). For each cell at the indicated pH ($n = 7$ cells), I_{Ba} was normalized to the peak amplitude of I_{Ba} at pH 7.3 and plotted against test voltage as the mean (line) ± SEM (shaded region). (b-e) Parameters from Boltzmann fits of I-V data in *(a)* plotted against extracellular pH (V_h, *b*; G_{max}, *c*; *k*, *d*; and V_{rev}, *e*) as mean (symbols) ± SEM (bars) and fit by linear regression.

higher pH (Figure 2e). These results show that elevations in extracellular pH enhance activation and weaken the ion selectivity of $Ca_v1.4$ FL channels containing the $\beta_{2\times13}$ and $\alpha_2\delta$-4 subunits.

Distinct effects of CTD deletions on pH modulation of $Ca_v1.4$

Given that truncations of the CTD in $Ca_v1.4\Delta e47$ and K1591X cause hyperpolarizing shifts in the voltage-dependence of activation [22–24,26], we hypothesized that these variants might be more resistant to the effects of alkalinization. To test this, we analyzed the effects of increasing pH on I_{Ba} in cells transfected with $Ca_v1.4\Delta e47$ (Figure 3a–e) or K1591X (Figure 4a–e). As was the case for $Ca_v1.4$ FL, alkalinization caused a significant hyperpolarization of V_h and V_{rev} as well as an increase in G_{max} for $Ca_v1.4\Delta e47$ and K1591X. However, the modest pH-dependent decline in k (i.e. slope of the linear regression line was significantly non-zero) was only seen for K1591X (Figure 4d) and $Ca_v1.4$ FL (Figure 2d) but not $Ca_v1.4\Delta e47$ (Figure 3d).

To further characterize the differences in the $Ca_v1.4$ variants, the % change in I_{Ba} relative to that at pH 7.3 was fit by the Hill equation (Figure 5a,b). With this analysis, the stronger pH sensitivity of $Ca_v1.4$ FL was

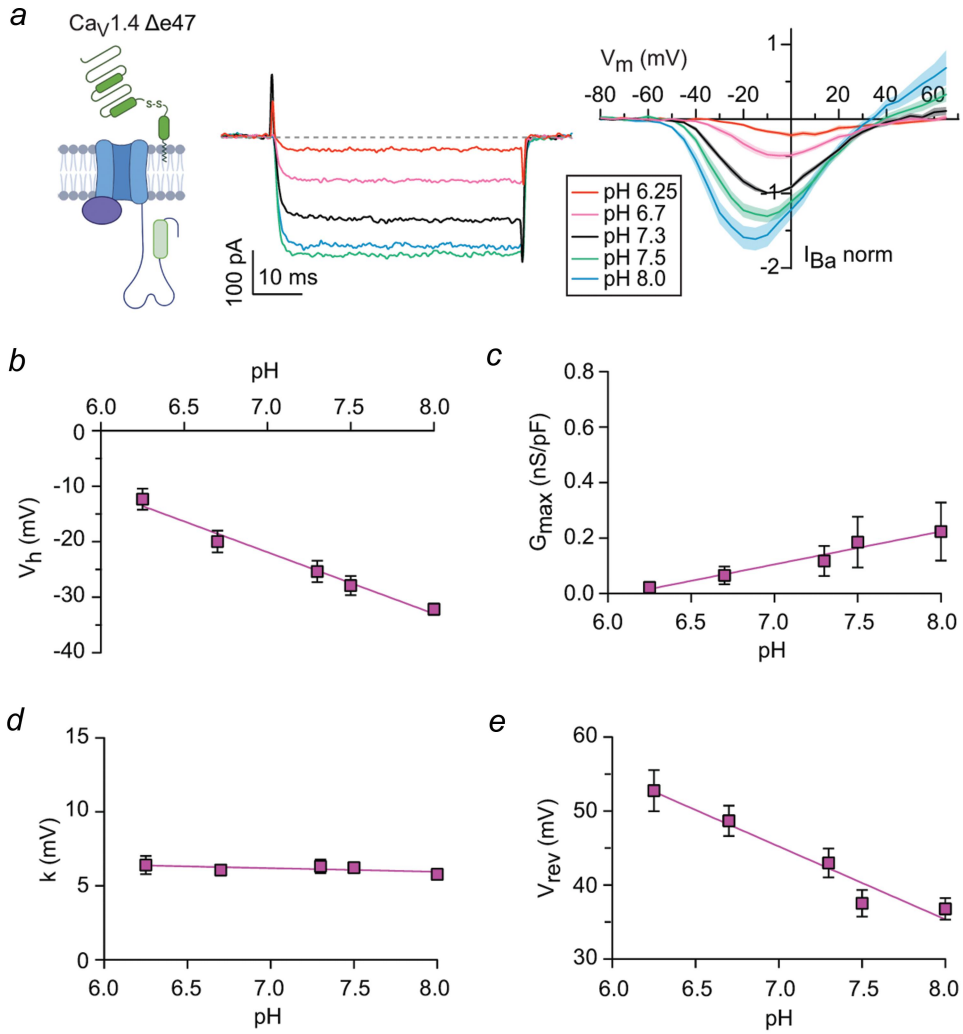

Figure 3. pH-dependent modulation of I_{Ba} in cells transfected with Ca$_V$1.4Δe47. (a) Representative traces and I-V plot for I_{Ba} elicited by 50-ms pulses from −80 mV to various voltages. Current traces represent I_{Ba} in a single cell evoked by test pulses evoking the peak I_{Ba} at the indicated pH values (with increasing pH: −5, −5, −10, −15 and −15 mV). For each cell at the indicated pH ($n = 5$ cells), I_{Ba} was normalized to the peak amplitude of I_{Ba} at pH 7.3 and plotted against test voltage as the mean (line) ± SEM (shaded region). (b-e) Parameters from Boltzmann fits of I-V data in *(a)* plotted against extracellular pH (V_h, *b*; G_{max}, *c*; *k*, *d*; and V_{rev}, *e*) as mean (symbols) ± SEM (bars) and fit by linear regression.

evident as a lower IC_{50} for proton inhibition compared to Ca$_v$1.4Δe47, which did not reach statistical significance for K1591X, and significantly steeper slope than for both variants (Figure 5c). Notably, the pH-dependent change in I_{Ba} was higher for Ca$_v$1.4 FL than for Ca$_v$1.4Δe47 and K1591X at elevated pH (>7.3) with little difference at low pH (<7.3, Figure 5b). Analyses of the pH-dependence of the I-V parameters (Figure 6a–e) indicated that the stronger pH-dependent modulation of I_{Ba} for Ca$_v$1.4 FL was mainly due to a greater sensitivity of G_{max} to pH changes (Figure 6b,e). These results suggest that deletions of the CTD that enhance activation minimize the impact of pH changes on Ca$_v$1.4-mediated currents.

$\alpha_2\delta$ subunits modulate the impact of pH on Ca$_v$1.4 FL but not Ca$_v$1.4Δe47 or K1591X

A previous study showed that Ca$_v$1.4 was more sensitive to inhibition by low pH than potentiation by high pH [9]. In contrast, we found that each of the Ca$_v$1.4 variants were strongly modulated by both low and high pH (Figures 2–4). A potential source of the

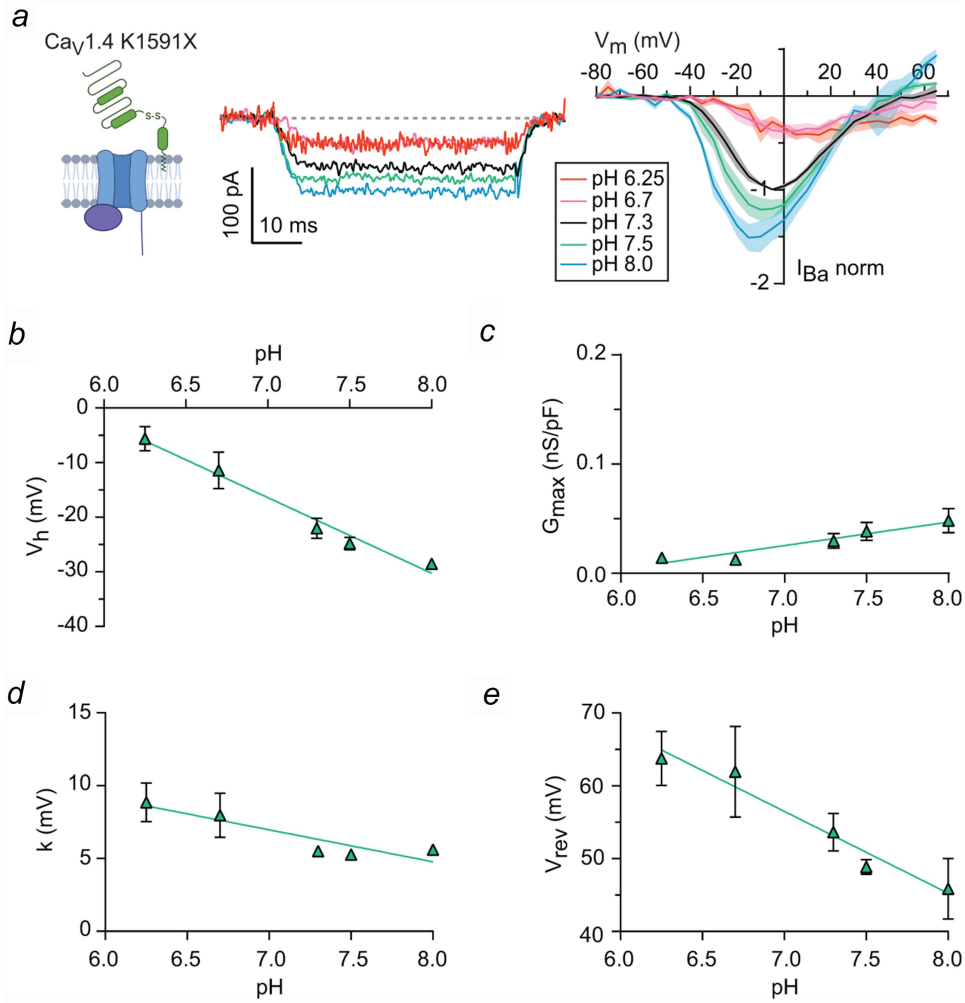

Figure 4. pH-dependent modulation of I_{Ba} in cells transfected with K1591X. (a) Representative traces and I-V plot for I_{Ba} elicited by 50-ms pulses from −80 mV to various voltages. Current traces represent I_{Ba} in a single cell evoked by test pulses evoking the peak I_{Ba} at the indicated pH values (with increasing pH: +15, 0, −5, −5 and −15 mV). For each cell at the indicated pH ($n = 4$ cells), I_{Ba} was normalized to the peak amplitude of I_{Ba} at pH 7.3 and plotted against test voltage as the mean (line) ± SEM (shaded region). (b-e) Parameters from Boltzmann fits of I-V data in *(a)* plotted against extracellular pH (V_h, *b*; G_{max}, *c*; *k*, *d*; and V_{rev}, *e*) as mean (symbols) ± SEM (bars). Line represents fit by linear regression.

discrepancy is that we reconstituted the channels with $\alpha_2\delta$-4 whereas the prior study used $\alpha_2\delta$-1. Thus, we compared pH modulation of $Ca_V1.4$ FL in cells co-transfected with $\alpha_2\delta$-4 or $\alpha_2\delta$-1, or without any $\alpha_2\delta$ (Figure 7a–h). Although the identity of the $\alpha_2\delta$ did not affect I-V parameters (Table 1), I_{Ba} underwent significantly less potentiation by high pH for $Ca_V1.4$ FL with $\alpha_2\delta$-1 than with $\alpha_2\delta$-4 (Figure 7a,c,h). This could be explained by a weaker pH-dependence of V_h, G_{max}, and k without a change in V_{rev} (Figure 7d–h). Interestingly, the pH regulation of $Ca_V1.4$ FL with $\alpha_2\delta$-1 was not different from channels without any $\alpha_2\delta$ (Figure 7b–h). In contrast to these findings for $Ca_V1.4$ FL, the co-expression of $\alpha_2\delta$-1 or lack of $\alpha_2\delta$ did not greatly affect the pH-dependence of I-V parameters for $Ca_v1.4\Delta e47$ (Figure 8a–h) and had modest effects on K1591X (Figure 9a–h). These results suggest a unique ability of $\alpha_2\delta$-4 to promote pH modulation of $Ca_V1.4$ FL and to a lesser extent K1591X, but not $Ca_v1.4\Delta e47$.

Discussion

Our study provides new insights about pH-mediated regulation of $Ca_V1.4$ channels. First, we demonstrate that $Ca_V1.4$ FL channels containing

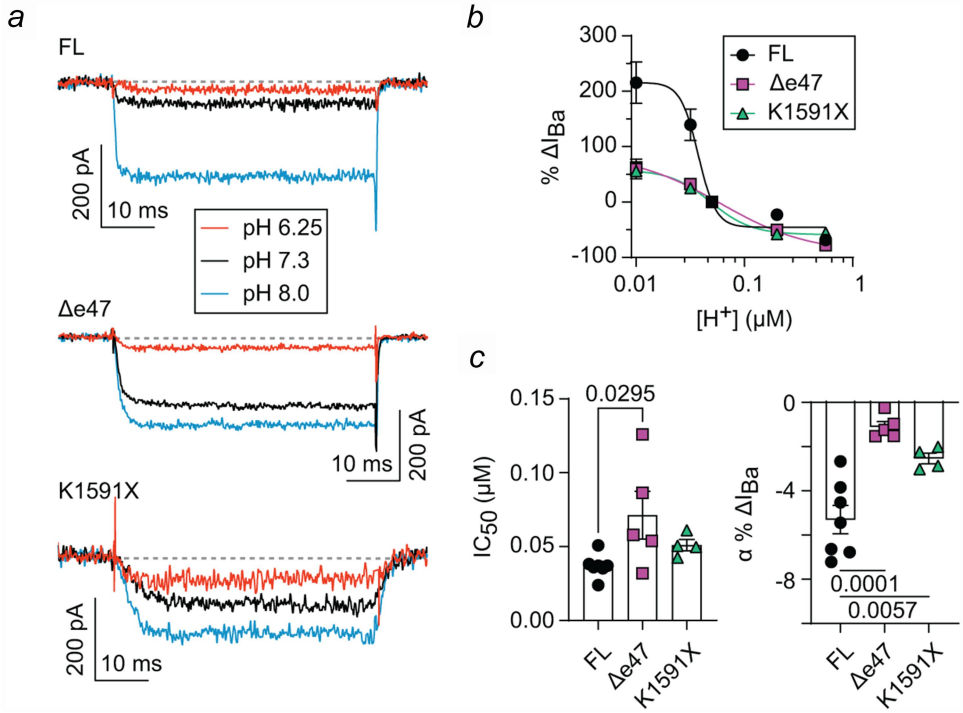

Figure 5. Weaker pH modulation of $Ca_V1.4\Delta e47$ and K1591X than $Ca_V1.4$ FL. (a) Representative traces for I_{Ba} elicited by 50-ms pulses from −80 mV to voltages evoking the peak I_{Ba} at the indicated pH values (with increasing pH: +10, +5 and −10 mV) in cells expressing $Ca_V1.4$ FL ($n = 7$ cells), $Ca_V1.4\Delta e47$ ($n = 5$ cells), or K1591X ($n = 4$ cells). (b) I_{Ba} evoked as in *(a)* was expressed as % difference from I_{Ba} at pH 7.3 (% ΔI_{Ba}) and plotted against extracellular $[H^+]$ in μM as mean (symbols) ± SEM (bars). Line represents fit by Hill equation. (c) IC_{50} and slope (α) determined by nonlinear fits of data in (b). Columns and bars represent mean ± SEM. Significant differences between groups (p-values shown above) were determined by one-way ANOVA ($F(2,13) = 3.853$, overall $p = 0.0485$ for IC_{50}; $F(2,13) = 18.53$, overall $p = 0.0002$ for α) and post-hoc Dunnett's test.

$\beta_{2\times13}$ and $\alpha_2\delta$-4 are strongly modulated by pH in HEK293T cells as has been reported for these channels at photoreceptor synapses [10,28]. Second, we uncover a key role for the CTD in controlling pH sensitivity of $Ca_V1.4$ FL in that truncations of the CTD reduce the responsiveness of $Ca_V1.4$ Δe47 and K1591X to pH. Finally, we show that $\alpha_2\delta$-4 confers stronger pH modulation than $\alpha_2\delta$-1, but this effect requires an intact CTD since $Ca_v1.4\Delta e47$ and K1591X exhibit less preference for a specific $\alpha_2\delta$ with respect to their pH sensitivity. These findings reveal unexpected roles for $\alpha_2\delta$ subunits and the CTD in fine-tuning the responsiveness of $Ca_v1.4$ to fluctuations in extracellular pH.

C-terminal variation of $Ca_v1.4$ and pH modulation

Extracellular acidification decreases current amplitudes and causes positive shifts in the I-V relationships of all Ca_v channels [9]. Proposed mechanisms for these effects include protons competing with Ca^{2+} for binding to the selectivity filter and the neutralization of surface charges, respectively [29–32]. Protonation of selectivity residues could account for pH-dependent changes in V_{rev} that were seen for each $Ca_v1.4$ variant (Figures 2e,3e,4e). However, there remains some controversy regarding which protonation sites mediate pH modulation of Ca_v channels [29,30,33,34]. Moreover, differences in the pH sensitivity of the various Ca_v subtypes suggest that additional mechanisms may be involved. For example, under identical recording conditions, Ca_v3 channels show stronger regulation by low pH compared to Ca_v1 and Ca_v2 channels [9]. Similarly, we found that while I_{Ba} for $Ca_v1.4$ FL, $Ca_v1.4\Delta e47$, and K1591X are all strongly modulated by extracellular pH (Figures 2–4), they differ in their responses (Figures 5–6). The increase in I_{Ba} by high pH was larger for $Ca_v1.4$ FL than for $Ca_v1.4\Delta e47$ and K1591X (Figure 5b), suggesting a role for the CTD in adjusting the pH sensitivity of the channel.

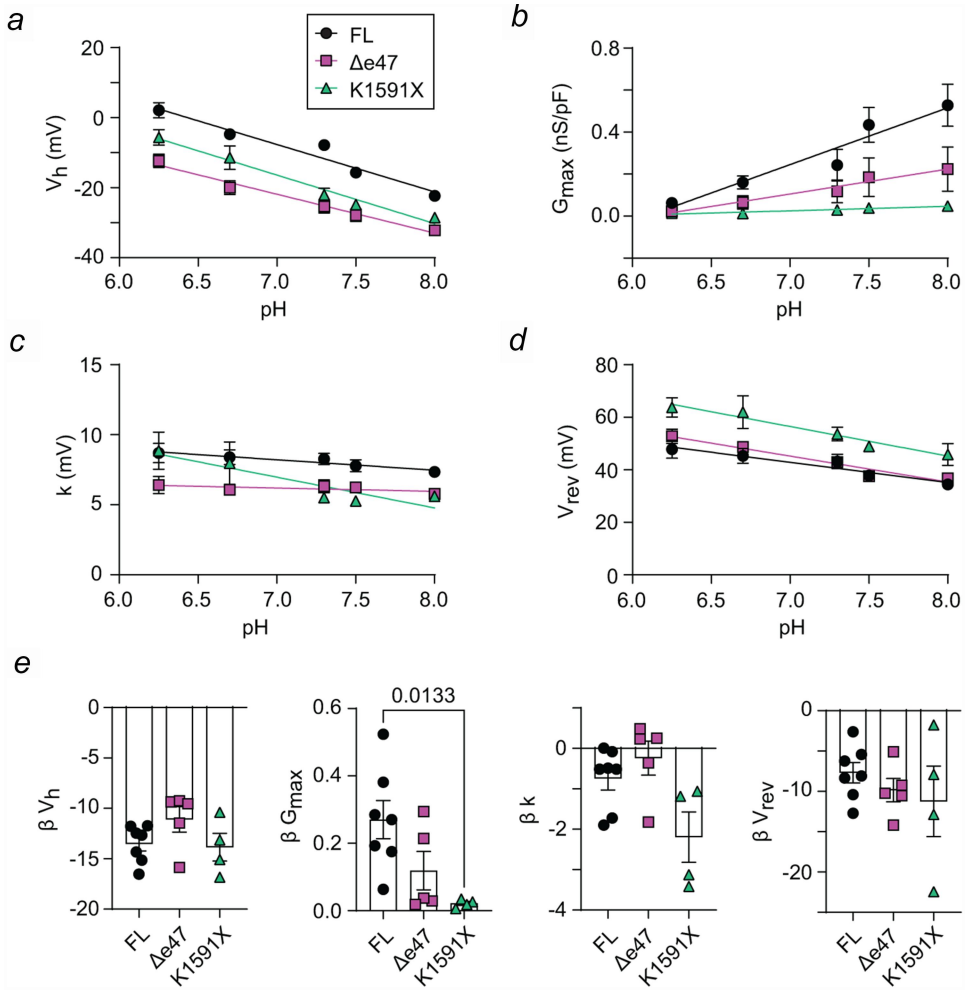

Figure 6. G_{max} for K1591X shows little pH-dependence compared to $Ca_v1.4\Delta e47$ and $Ca_v1.4$ FL. (a-d) Boltzmann parameters from I-V data in Figures 1–3 plotted against extracellular pH. Symbols and bars that represent mean ± SEM. Lines represent fit by linear regression. (e) Slopes (β) of the linear fits in (a-d). Bars represent mean ± SEM. By one-way ANOVA or Kruskal-Wallis test, there was a significant difference in β G_{max} ($F(2,13) = 5.532$, $p = 0.018$) but no significant difference in β V_h ($H(2) = 3.977$, $p = 0.1366$) or β V_{rev} ($F(2,13) = 0.6689$, $p = 0.5290$). p-value for β G_{max} shown for K1591X vs FL was determined by post-hoc Dunnett's test. By one-way ANOVA, there was a significant overall difference in β k ($F(2,13) = 5.041$, $p = 0.0240$), but no difference by post-hoc Dunnett's test.

We expected that the negative shifts in V_h for $Ca_v1.4\Delta e47$ and K1591X might occlude the effects of pH on V_h. However, the V_h for $Ca_v1.4\Delta e47$ and K1591X showed a similar pH-dependence as for $Ca_v1.4$ FL (Figure 6a). For K1591X and to a lesser extent $Ca_v1.4\Delta e47$, the weaker effects of high pH on I_{Ba} could be attributed to a weaker pH-dependence of G_{max} (Figure 6b,e). pH-induced changes in G_{max} of Ca_v channels can be explained by alterations in single channel conductance [29,32]. However, disruption of the CTM is expected to increase the open probability (P_o) of Ca_v1 channels without affecting the single channel conductance [35,36]. The increase in P_o is thought to arise from the Ca^{2+}-free form of CaM (i.e. apo-CaM) bound to the IQ domain [36], which would be favored by our recording conditions since we used Ba^{2+} as a charge carrier. The increased P_o of $Ca_v1.4\Delta e47$ and K1591X could occlude further increases in P_o upon extracellular alkalinization. Structural changes induced by absence of the CTM could mimic channel conformations induced by high pH such that alkalinization has less of an effect in $Ca_v1.4\Delta e47$ and K1591X than in $Ca_v1.4$

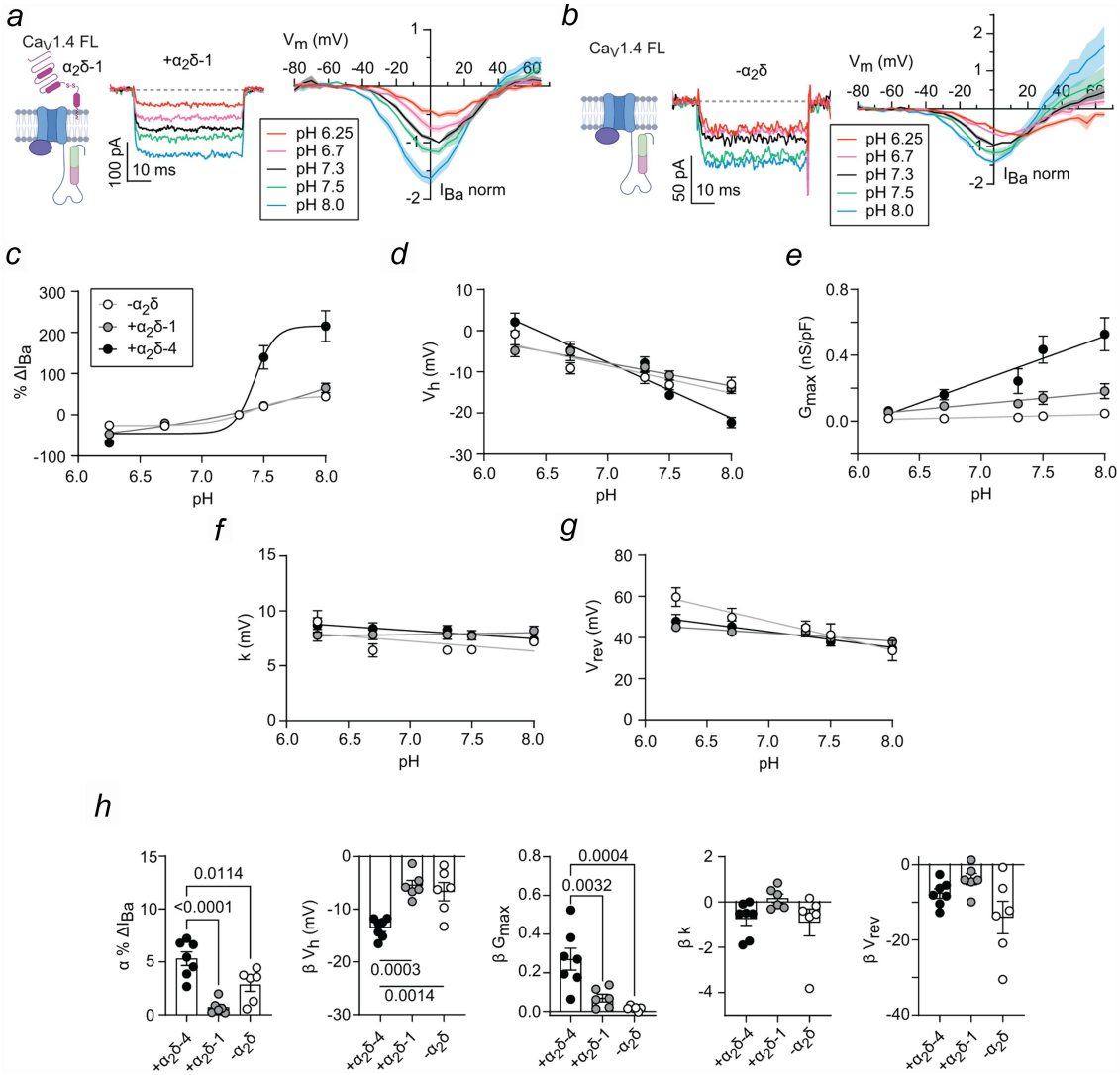

Figure 7. $\alpha_2\delta$-4 enhances pH-dependent modulation of $Ca_V1.4$ FL. (a,b) Representative traces and I-V plot for I_{Ba} elicited by 50-ms pulses from −80 mV to various voltages for $Ca_V1.4$ FL expressed with $\alpha_2\delta$-1 (a) or without any $\alpha_2\delta$ (b). Current traces correspond to voltages evoking the peak I_{Ba} at the indicated pH (with increasing pH: −5, −10, −15, −15 and −20 mV in *(a)* and 0, −10, −10, −15 and −15 mV in *(b)*). For each cell at the indicated pH (+$\alpha_2\delta$-1, $n = 6$ cells; -$\alpha_2\delta$, $n = 6$ cells), I_{Ba} was normalized to the peak amplitude of I_{Ba} at pH 7.3 and plotted against test voltage as the mean (line) ± SEM (shaded region). (c-g) % difference from I_{Ba} at pH 7.3 (% ΔI_{Ba}) (c) Boltzmann parameters were plotted against extracellular pH as mean (symbols) ± SEM (bars). Lines represent fit by Hill equation (c) or linear regression (d-g). (h) Slopes (α, β) of the fits in (c-g). Bars represent mean ± SEM. By one-way ANOVA, there was a significant difference in α for % ΔI_{Ba} ($F(2,16) = 17.38$, $p < 0.0001$), V_h ($F(2,16) = 14.14$, $p = 0.0003$), and G_{max} ($F(2,16) = 12.81$, $p = 0.0005$) but not V_{rev} ($F(2,16) = 3.674$, $p = 0.0486$). By Kruskal-Wallis test, there was a significant difference in β for k ($H(2) = 6.031$, $p = 0.0429$). p-values for significantly different groups are shown and determined by post-hoc Dunnett's test.

FL. Alternatively, the CTD might regulate the protonation of regions of the channel that control G_{max}. Since our experiments involved changes in extracellular pH, these residues are likely located on the extracellular side of the channel rather than within the cytoplasmic CTD itself. Cytoplasmic domains can trigger functional alterations involving extracellular facing regions of the channel. For example, Ca^{2+}-CaM binding of the CTD produces changes in selectivity filter that decrease G_{max} during CDI [37]. Similarly, the CTD of $Ca_v1.4$ FL may enable the dynamic protonation and deprotonation of external sites of the channel which could be less modifiable in the context of $Ca_v1.4\Delta e47$ and K1591X.

As is the case for $Ca_v1.4$, splice variation in the CTD of $Ca_v1.2$ and $Ca_v1.3$ can cause hyperpolarizing shifts in voltage-dependent activation

Table 1. I-V parameters at pH 7.3 for $Ca_V1.4$ channel variants expressed with $\alpha_2\delta$-4, $\alpha_2\delta$-1, or without $\alpha_2\delta$.

	+$\alpha_2\delta$-4	+$\alpha_2\delta$-1	-$\alpha_2\delta$	F (degrees freedom)	p value
$Ca_V1.4$ FL					
G_{max} (nS/pF)	0.24 ± 0.07	0.11 ± 0.02	0.02 ± 0.003*	F(2, 16) = 5.124	0.0191
V_h (mV)	−7.85 ± 1.47	−8.85 ± 1.31	−11.34 ± 1.51	F(2, 16) = 1.564	0.2397
k (mV)	8.27 ± 0.41	7.83 ± 0.43	6.42 ± 0.34*	H(2) = 7.523	0.0162
V_{rev} (mV)	43.15 ± 2.73	42.54 ± 2.25	44.83 ± 3.21	F(2, 16) = 0.1763	0.8400
$Ca_V1.4\Delta47$					
G_{max} (nS/pF)	0.12 ± 0.05	0.13 ± 0.03	0.05 ± 0.02	F(2, 11) = 1.167	0.3471
V_h (mV)	−25.34 ± 1.93	−28.20 ± 0.63	−22.06 ± 1.26$^{\&}$	F(2, 11) = 4.224	0.0435
k (mV)	6.32 ± 0.47	5.27 ± 0.26	5.60 ± 0.35	F(2, 11) = 1.908	0.1943
V_{rev} (mV)	42.98 ± 1.97	34.69 ± 2.47	29.38 ± 2.52**	F(2, 11) = 9.282	0.0043
$Ca_V1.4$ K1591X					
G_{max} (nS/pF)	0.03 ± 0.01	0.14 ± 0.05	0.01 ± 0.001$^{\&}$	H(2) = 9.052	0.0018
V_h (mV)	−22.001 ± 1.86	−25.41 ± 1.10	−22.14 ± 0.67	F(2, 11) = 2.268	0.1498
k (mV)	5.50 ± 0.15	6.18 ± 0.23	6.58 ± 0.83	H(2) = 2.978	0.2412
V_{rev} (mV)	53.63 ± 2.58	33.25 ± 0.68***	53.23 ± 5.84$^{\&\&\&}$	F(2, 11) = 25.89	<0.0001

Boltzmann parameters from I-V data from Figures 1a, 2a, 3a, 6a,b, 7a,b, 8a,b are reported as mean ± SEM. F-statistic and p-values were determined by one-way ANOVA or Kruskal-Wallis test. Significantly different groups were determined by post-hoc Tukey's or Dunn's multiple comparisons tests: *$p < 0.05$, **$p < 0.05$, ***$p < 0.001$ compared to +α2δ-4; $^{\&}p < 0.05$, $^{\&\&\&}p < 0.001$ compared to +α2δ-1.

[35,38–40]. Both Ca_v1 subtypes are expressed in the brain and the heart where they regulate neuronal and cardiac excitability, respectively [41]. Like $Ca_v1.4\Delta e47$, $Ca_v1.2$ and $Ca_v1.3$ C-terminal splice variants exhibiting negative activation thresholds are expected to be less sensitive to fluctuations in pH that occur in response to injury and disease [42,43]. Thus, studying the mechanisms whereby the CTD modifies pH sensitivity of Ca_v1 channels could help guide development of novel strategies to pharmacologically target these channels in various physiological contexts.

A role for $\alpha_2\delta$ in regulating the pH sensitivity of $Ca_V1.4$ FL

$\alpha_2\delta$ subunits are large proteins that are anchored to the plasma membrane and bind to extracellular sites in the pore-forming α_1 subunit [44–46]. For some Ca_v subtypes, this interaction enhances the voltage-dependence of activation by increasing the sensitivity of voltage sensor domains and their coupling to the pore [47,48]. Since the identity of the $\alpha_2\delta$ subunit did not affect voltage-dependent activation of $Ca_v1.4$ (Table 1), differences in the impact of $\alpha_2\delta$-1 and $\alpha_2\delta$-4 on pH modulation of $Ca_v1.4$ are unlikely to arise from their differential coupling to voltage-sensing and/or pore opening. Compared to $\alpha_2\delta$-1, $\alpha_2\delta$-4 lacks key residues important for binding to gabapentinoid drugs [49]. In addition, the metal ion dependent adhesion site in the von Willebrand A domain of $\alpha_2\delta$-4 differs from that of $\alpha_2\delta$-1 in lacking a polar residue [50,51]. These amino acid differences could reveal and/or modify protonation sites in the channel complex that could account for the unique effects of $\alpha_2\delta$-4 on enhancing pH-dependent modulation of $Ca_v1.4$ as well as K1591X.

Potential significance of distinct pH modulation of $Ca_V1.4$ FL, $Ca_V1.4\Delta e47$, and K1591X

Vision depends on transmission of light information from photoreceptors to horizontal and bipolar cells [52]. This process requires Ca_v 1.4-dependent glutamate release from photoreceptors. Horizontal cells regulate the gain of photoreceptor synapses in a manner that generates the center-surround receptive field characteristics of bipolar cells and retinal ganglion cells [53,54]. For example, light-dependent hyperpolarization of cones in the surround portion of an ON bipolar cell's receptive field augments the impact of darkness in the center of its receptive field. Recent evidence suggests that hyperpolarization of horizontal cells in the surround leads to alkalinization of the center cone synapse by inhibiting the electrogenic bicarbonate transporter, SLC4a5, in horizontal cell dendritic tips [55]. The subsequent hyperpolarization of the V_h of cone $Ca_v1.4$ channels then leads to an

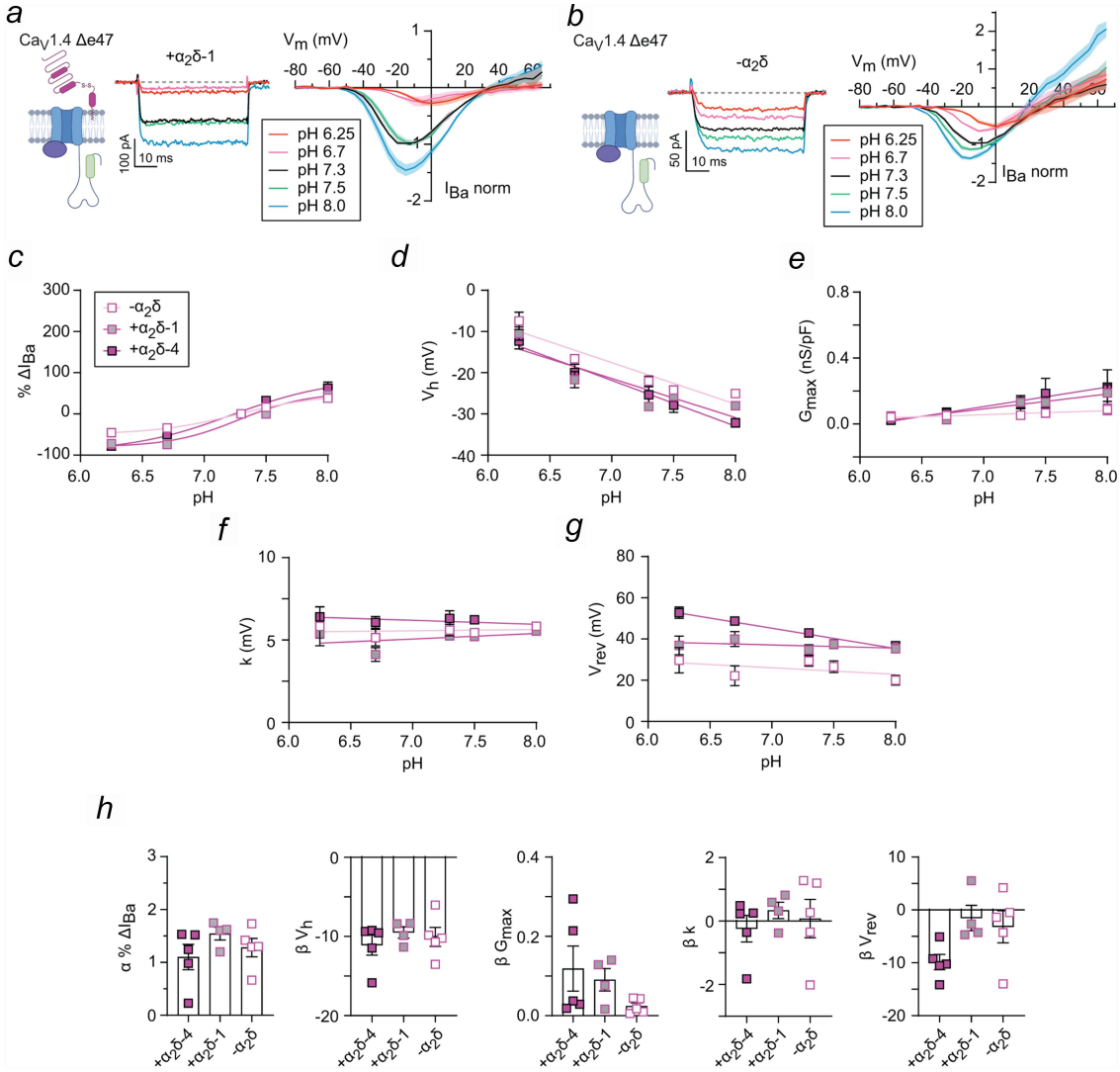

Figure 8. $\alpha_2\delta$ subunits do not enhance pH-dependent modulation of $Ca_V1.4$ Δe47.Representative traces and I-V plot for I_{Ba} elicited by 50-ms pulses from −80 mV to various voltages for $Ca_V1.4$ Δe47 expressed with $\alpha_2\delta$-1 (a) or without any $\alpha_2\delta$ (b). Current traces correspond to voltages evoking the peak I_{Ba} at the indicated pH (with increasing pH: −5, −10, −15, −15 and −20 mV in *(a)* and 0, −10, −10, −15 and −15 mV in *(b)*). For each cell at the indicated pH (+$\alpha_2\delta$-1, $n = 4$ cells; -$\alpha_2\delta$, $n = 5$ cells), I_{Ba} was normalized to the peak amplitude of I_{Ba} at pH 7.3 and plotted against test voltage as the mean (line) ± SEM (shaded region). (c-g) % difference from I_{Ba} at pH 7.3 (% ΔI_{Ba}) (c) and Boltzmann parameters were plotted against extracellular pH as mean (symbols) ± SEM (bars). Lines represent fit by Hill equation (c) or linear regression (d-g). (h) Slopes (α, β) of the fits in (c-g). Bars represent mean ± SEM. By one-way ANOVA, there was not a significant difference in α for % ΔI_{Ba} ($F(2,11) = 1.240$, $p = 0.3269$), G_{max} ($F(2,11) = 1.7$, $p = 0.2274$), k ($F(2,11) = 0.3577$, $p = 0.7071$), and V_{rev} ($F(2,11) = 3.415$, $p = 0.0702$). By Kruskal-Wallis test, there was not a significant difference in β for V_h ($H(2) = 0.7257$, $p = 0.7287$).

increase in glutamate release that augments the effect of darkness in suppressing the activity of the ON bipolar cell [16,56–58]. Compared to $Ca_v1.4$ FL, the weaker pH sensitivity of $Ca_V1.4\Delta e47$ may adjust horizontal cell feedback in particular regions of the retina and/or at a particular developmental timepoint. For K1591X, the reduced pH-sensitivity of G_{max} could contribute to aberrant horizontal cell feedback that could underlie reductions in contrast sensitivity and/or color vision reported in many cases of CSNB2 [59,60]. An understanding of

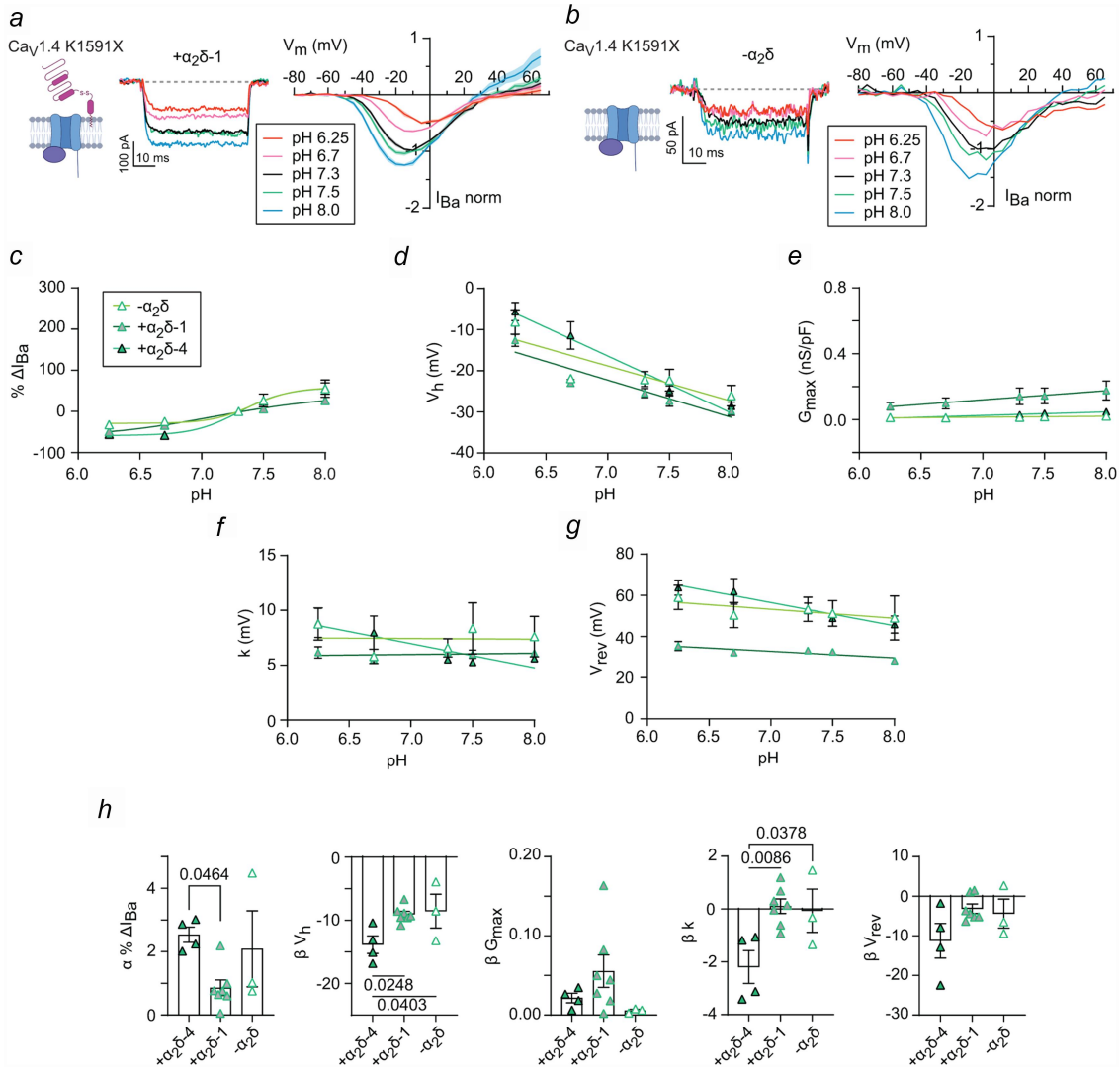

Figure 9. $\alpha_2\delta$-4 enhances pH-dependent modulation of K1591X. Representative traces and I-V plot for I_{Ba} elicited by 50-ms pulses from −80 mV to various voltages for $Ca_V1.4$ K1591X expressed with $\alpha_2\delta$-1 (a) or without any $\alpha_2\delta$ (b). Current traces correspond to voltages evoking the peak I_{Ba} at the indicated pH (with increasing pH: −5, −10, −15, −15 and −20 mV in *(a)* and 0, −10, −10, −15 and −15 mV in *(b)*). For each cell at the indicated pH (+$\alpha_2\delta$-1, $n = 7$ cells; -$\alpha_2\delta$, $n = 3$ cells), I_{Ba} was normalized to the peak amplitude of I_{Ba} at pH 7.3 and plotted against test voltage as the mean (line) ± SEM (shaded region). (c-g) % difference from I_{Ba} at pH 7.3 (% ΔI_{Ba}) (c) and Boltzmann parameters were plotted against extracellular pH as mean (symbols) ± SEM (bars). Lines represent fit by Hill equation (c) or linear regression (d-g). (h) Slopes (α, β) of the fits in (c-g). Bars represent mean ± SEM. By one-way ANOVA, there was a significant difference in α for % ΔI_{Ba} ($F(2,11) = 3.725$, $p = 0.0582$), V_h ($F(2,11) = 5.156$, $p = 0.0263$), and Δk ($F(2,11) = 6.740$, $p = 0.0123$) but not G_{max} ($F(2,11) = 1.903$, $p = 0.1951$) nor V_{rev} ($F(2,11) = 2.575$, $p = 0.1210$). p-values for significantly different groups are shown and determined by post-hoc Dunnett's test.

how normal and pathological variations in the CTD of $Ca_v1.4$ modify photoreceptor synaptic output and visual processing remains an important challenge for future studies.

Conceptualization, J.D.V., A.L.; Methodology, J.D.V., A.L. Investigation, J.D.V.; Writing – original draft, J.D.V., A.L.; Writing – review and editing, J.D.V., A.L. Funding acquisition, A.L. All authors have read and approved the manuscript.

Acknowledgments

The authors thank J. Sun for assistance with cell culture maintenance.

Disclosure statement

No potential conflict of interest was reported by the author(s).

Author contributions

CRediT: **Juan de la Rosa Vázquez:** Conceptualization, Formal analysis, Investigation, Validation, Writing – original draft, Writing – review & editing; **Amy Lee:** Conceptualization, Formal analysis, Funding acquisition, Project administration, Resources, Writing – original draft, Writing – review & editing.

Funding

This work was supported by grants from the National Institutes of Health [EY026817, TR005086] and startup funds from The University of Texas at Austin.

Data availability statement

The data that support the findings of this study are available from the corresponding author, A.L., upon request.

ORCID

Juan de la Rosa Vázquez http://orcid.org/0000-0002-6266-5919
Amy Lee http://orcid.org/0000-0001-8021-0443

References

[1] Hung CH, Chin Y, Fong YO, et al. Acidosis-related pain and its receptors as targets for chronic pain. Pharmacol Ther. 2023;247:108444. doi: 10.1016/j.pharmthera.2023.108444
[2] Quade BN, Parker MD, Occhipinti R. The therapeutic importance of acid-base balance. Biochem Pharmacol. 2021;183:114278. doi: 10.1016/j.bcp.2020.114278
[3] Miesenbock G, De Angelis DA, Rothman JE. Visualizing secretion and synaptic transmission with pH-sensitive green fluorescent proteins. Nature. 1998;394(6689):192–195. doi: 10.1038/28190
[4] von Hanwehr R, Smith ML, Siesjo BK. Extra- and intracellular pH during near-complete forebrain ischemia in the rat. J Neurochem. 1986;46(2):331–339. doi: 10.1111/j.1471-4159.1986.tb12973.x
[5] Krishtal OA, Osipchuk YV, Shelest TN, et al. Rapid extracellular pH transients related to synaptic transmission in rat hippocampal slices. Brain Res. 1987;436(2):352–356. doi: 10.1016/0006-8993(87)91678-7
[6] Palmer MJ, Hull C, Vigh J, et al. Synaptic cleft acidification and modulation of short-term depression by exocytosed protons in retinal bipolar cells. J Neurosci. 2003;23(36):11332–11341. doi: 10.1523/JNEUROSCI.23-36-11332.2003
[7] Prole DL, Lima PA, Marrion NV. Mechanisms underlying modulation of neuronal KCNQ2/KCNQ3 potassium channels by extracellular protons. J Gen Physiol. 2003;122(6):775–793. doi: 10.1085/jgp.200308897
[8] Traynelis SF, Cull-Candy SG. Pharmacological properties and H+ sensitivity of excitatory amino acid receptor channels in rat cerebellar granule neurones. J Physiol. 1991;433(1):727–763. doi: 10.1113/jphysiol.1991.sp018453
[9] Doering CJ, McRory JE. Effects of extracellular pH on neuronal calcium channel activation. Neuroscience. 2007;146(3):1032–1043. doi: 10.1016/j.neuroscience.2007.02.049
[10] DeVries SH. Exocytosed protons feedback to suppress the Ca2+ current in mammalian cone photoreceptors. Neuron. 2001;32(6):1107–1117. doi: 10.1016/S0896-6273(01)00535-9
[11] Cho S, von Gersdorff H. Proton-mediated block of Ca2+ channels during multivesicular release regulates short-term plasticity at an auditory hair cell synapse. J Neurosci. 2014;34(48):15877–15887. doi: 10.1523/JNEUROSCI.2304-14.2014
[12] Vessey JP, Stratis AK, Daniels BA, et al. Proton-mediated feedback inhibition of presynaptic calcium channels at the cone photoreceptor synapse. J Neurosci. 2005;25(16):4108–4117. doi: 10.1523/JNEUROSCI.5253-04.2005
[13] Snellman J, Mehta B, Babai N, et al. Acute destruction of the synaptic ribbon reveals a role for the ribbon in vesicle priming. Nat Neurosci. 2011;14(9):1135–1141. doi: 10.1038/nn.2870
[14] Vincent PFY, Cho S, Tertrais M, et al. Clustered Ca(2+) channels are blocked by synaptic vesicle proton release at mammalian auditory ribbon synapses. Cell Rep. 2018;25(12):3451–3464.e3. doi: 10.1016/j.celrep.2018.11.072
[15] Barnes S, Merchant V, Mahmud F. Modulation of transmission gain by protons at the photoreceptor output synapse. Proc Natl Acad Sci USA. 1993;90(21):10081–10085. doi: 10.1073/pnas.90.21.10081
[16] Barnes S, Bui Q. Modulation of calcium-activated chloride current via pH-induced changes of calcium channel properties in cone photoreceptors. J Neurosci. 1991;11(12):4015–4023. doi: 10.1523/JNEUROSCI.11-12-04015.1991
[17] Hirasawa H, Kaneko A. pH changes in the invaginating synaptic cleft mediate feedback from horizontal cells to cone photoreceptors by modulating Ca2+ channels. J Gen Physiol. 2003;122(6):657–671. doi: 10.1085/jgp.200308863
[18] Verweij J, Kamermans M, Spekreijse H. Horizontal cells feed back to cones by shifting the cone calcium-current activation range. Vision Res. 1996;36(24):3943–3953. doi: 10.1016/S0042-6989(96)00142-3
[19] Barnes S. Center-surround antagonism mediated by proton signaling at the cone photoreceptor synapse. J Gen Physiol. 2003;122(6):653–656. doi: 10.1085/jgp.200308947
[20] Williams B, Maddox JW, Lee A. Calcium channels in retinal function and disease. Annu Rev Vis Sci. 2022;8(1):53–77. doi: 10.1146/annurev-vision-012121-111325
[21] Lee A, Wang S, Williams B, et al. Characterization of Cav1.4 complexes (α11.4, β2, and α2δ4) in HEK293T

cells and in the retina. J Biol Chem. 2015;290 (3):1505–1521. doi: 10.1074/jbc.M114.607465

[22] Tan GM, Yu D, Wang J, et al. Alternative splicing at C terminus of $Ca_v.4$ calcium channel modulates calcium-dependent inactivation, activation potential, and current density. J Biol Chem. 2012;287 (2):832–847. doi: 10.1074/jbc.M111.268722

[23] Haeseleer F, Williams B, Lee A. Characterization of C-terminal splice variants of $Ca_v.4$ Ca^{2+} channels in human retina. J Biol Chem. 2016;291(30):15663–15673. doi: 10.1074/jbc.M116.731737

[24] Singh A, Hamedinger D, Hoda JC, et al. C-terminal modulator controls Ca^{2+}-dependent gating of $Ca_v.4$ L-type Ca^{2+} channels. Nat Neurosci. 2006;9(9):1108–1116. doi: 10.1038/nn1751

[25] Wahl-Schott C, Baumann L, Cuny H, et al. Switching off calcium-dependent inactivation in L-type calcium channels by an autoinhibitory domain. Proc Natl Acad Sci USA. 2006;103(42):15657–15662. doi: 10.1073/pnas.0604621103

[26] Williams B, Haeseleer F, Lee A. Splicing of an automodulatory domain in $Ca_v.4$ Ca^{2+} channels confers distinct regulation by calmodulin. J Gen Physiol. 2018;150(12):1676–1687. doi: 10.1085/jgp.201812140

[27] Williams B, Lopez JA, Maddox JW, et al. Functional impact of a congenital stationary night blindness type 2 mutation depends on subunit composition of $Ca_v.4$ Ca^{2+} channels. J Biol Chem. 2020;295(50):17215–17226. doi: 10.1074/jbc.RA120.014138

[28] Grove JCR, Hirano AA, de Los Santos J, et al. Novel hybrid action of GABA mediates inhibitory feedback in the mammalian retina. PLOS Biol. 2019;17(4): e3000200. doi: 10.1371/journal.pbio.3000200

[29] Chen XH, Bezprozvanny I, Tsien RW. Molecular basis of proton block of L-type Ca^{2+} channels. J Gen Physiol. 1996;108(5):363–374. doi: 10.1085/jgp.108.5.363

[30] Chen XH, Tsien RW. Aspartate substitutions establish the concerted action of P-region glutamates in repeats *I* and *III* in forming the protonation site of L-type Ca^{2+} channels. J Biol Chem. 1997;272(48):30002–30008. doi: 10.1074/jbc.272.48.30002

[31] Smirnov SV, Knock GA, Belevych AE, et al. Mechanism of effect of extracellular pH on L-type Ca^{2+} channel currents in human mesenteric arterial cells. Am J Physiol Heart Circ Physiol. 2000;279(1): H76–85. doi: 10.1152/ajpheart.2000.279.1.H76

[32] Delisle BP, Satin J. pH modification of human T-type calcium channel gating. Biophys J. 2000;78 (4):1895–1905. doi: 10.1016/S0006-3495(00)76738-5

[33] Cens T, Rousset M, Charnet P. Two sets of amino acids of the domain I of $Ca_v.3$ Ca^{2+} channels contribute to their high sensitivity to extracellular protons. Pflugers Arch. 2011;462 (2):303–314. doi: 10.1007/s00424-011-0974-x

[34] Prod'hom B, Pietrobon D, Hess P. Direct measurement of proton transfer rates to a group controlling the dihydropyridine-sensitive Ca^{2+} channel. Nature. 1987;329(6136):243–246. doi: 10.1038/329243a0

[35] Bock G, Gebhart M, Scharinger A, et al. Functional properties of a newly identified C-terminal splice variant of $Ca_v.3$ L-type Ca^{2+} channels. J Biol Chem. 2011;286 (49):42736–42748. doi: 10.1074/jbc.M111.269951

[36] Adams PJ, Ben-Johny M, Dick IE, et al. Apocalmodulin itself promotes ion channel opening and Ca(2+) regulation. Cell. 2014;159(3):608–622. doi: 10.1016/j.cell.2014.09.047

[37] Abderemane-Ali F, Findeisen F, Rossen ND, et al. A selectivity filter gate controls voltage-gated calcium channel calcium-dependent inactivation. Neuron. 2019;101 (6):1134–1149.e3. doi: 10.1016/j.neuron.2019.01.011

[38] Tan BZ, Jiang F, Tan MY, et al. Functional characterization of alternative splicing in the C terminus of L-type CaV1.3 channels. J Biol Chem. 2011;286 (49):42725–42735. doi: 10.1074/jbc.M111.265207

[39] Soldatov NM, Zühlke RD, Bouron A, et al. Molecular structures involved in L-type calcium channel inactivation - role of the carboxyl-terminal region encoded by exons 40–42 in α_{1C} subunit in the kinetics and Ca^{2+} dependence of inactivation. JBiolChem. 1997;272(6):3560–3566. doi: 10.1074/jbc.272.6.3560

[40] Tang ZZ, Liang MC, Lu S, et al. Transcript scanning reveals novel and extensive splice variations in human L-type voltage-gated calcium channel, Cav1.2 α1 subunit. J Biol Chem. 2004;279(43):44335–44343. doi: 10.1074/jbc.M407023200

[41] Zamponi GW, Striessnig J, Koschak A, et al. The physiology, pathology, and pharmacology of voltage-gated calcium channels and their future therapeutic potential. Pharmacol Rev. 2015;67(4):821–870. doi: 10.1124/pr.114.009654

[42] Chesler M. Regulation and modulation of pH in the brain. Physiol Rev. 2003;83(4):1183–1221. doi: 10.1152/physrev.00010.2003

[43] Gorodetsky AA, Kirilyuk IA, Khramtsov VV, et al. Functional electron paramagnetic resonance imaging of ischemic rat heart: monitoring of tissue oxygenation and pH. Magn Reson Med. 2016;76(1):350–358. doi: 10.1002/mrm.25867

[44] Davies A, Kadurin I, Alvarez-Laviada A, et al. The α 2 δ subunits of voltage-gated calcium channels form gpi-anchored proteins, a posttranslational modification essential for function. Proc Natl Acad Sci USA. 2010;107(4):1654–1659. doi: 10.1073/pnas.0908735107

[45] Cassidy JS, Ferron L, Kadurin I, et al. Functional exofacially tagged N-type calcium channels elucidate the interaction with auxiliary α2δ-1 subunits. Proc Natl Acad Sci USA. 2014;111(24):8979–8984. doi: 10.1073/pnas.1403731111

[46] Gurnett CA, Felix R, Campbell KP. Extracellular interaction of the voltage-dependent Ca2+ channel α2δ and α1 subunits. J Biol Chem. 1997;272(29):18508–18512. doi: 10.1074/jbc.272.29.18508

[47] Felix R, Gurnett CA, De Waard M, et al. Dissection of functional domains of the voltage-dependent Ca^{2+}

channel $\alpha_2\delta$ subunit. J Neurosci. 1997;17(18):6884–6891. doi: 10.1523/JNEUROSCI.17-18-06884.1997

[48] Savalli N, Pantazis A, Sigg D, et al. The α2δ-1 subunit remodels $Ca_V.2$ voltage sensors and allows Ca^{2+} influx at physiological membrane potentials. J Gen Physiol. 2016;148(2):147–159. doi: 10.1085/jgp.201611586

[49] Chen Z, Mondal A, Minor DL Jr. Structural basis for Ca_V α2δ: gabapentin binding. Nat Struct Mol Biol. 2023;30(6):735–739. doi: 10.1038/s41594-023-00951-7

[50] Dolphin AC. The α2δ subunits of voltage-gated calcium channels. Biochim Biophys Acta. 2013;1828 (7):1541–1549. doi: 10.1016/j.bbamem.2012.11.019

[51] Canti C, Nieto-Rostro M, Foucault I, et al. The metal-ion-dependent adhesion site in the Von Willebrand factor-A domain of $\alpha_2\delta$ subunits is key to trafficking voltage-gated Ca^{2+} channels. Proc Natl Acad Sci USA. 2005;102 (32):11230–11235. doi: 10.1073/pnas.0504183102

[52] Euler T, Haverkamp S, Schubert T, et al. Retinal bipolar cells: elementary building blocks of vision. Nat Rev Neurosci. 2014;15(8):507–519. doi: 10.1038/nrn3783

[53] Chaya T, Matsumoto A, Sugita Y, et al. Versatile functional roles of horizontal cells in the retinal circuit. Sci Rep. 2017;7(1):5540. doi: 10.1038/s41598-017-05543-2

[54] Stroh S, Puller C, Swirski S, et al. Eliminating glutamatergic input onto horizontal cells changes the dynamic range and receptive field organization of mouse retinal ganglion cells. J Neurosci. 2018;38(8):2015–2028. doi: 10.1523/JNEUROSCI.0141-17.2018

[55] Morikawa R, Rodrigues TM, Schreyer HM, et al. The sodium-bicarbonate cotransporter Slc4a5 mediates feedback at the first synapse of vision. Neuron. 2024;112(22):3715–3733.e9. doi: 10.1016/j.neuron.2024.08.015

[56] Wang TM, Holzhausen LC, Kramer RH. Imaging an optogenetic pH sensor reveals that protons mediate lateral inhibition in the retina. Nat Neurosci. 2014;17 (2):262–268. doi: 10.1038/nn.3627

[57] Liu X, Hirano AA, Sun X, et al. Calcium channels in rat horizontal cells regulate feedback inhibition of photoreceptors through an unconventional GABA- and pH-sensitive mechanism. J Physiol. 2013;591 (13):3309–3324. doi: 10.1113/jphysiol.2012.248179

[58] Thoreson WB, Mangel SC. Lateral interactions in the outer retina. Prog Retin Eye Res. 2012;31(5):407–441. doi: 10.1016/j.preteyeres.2012.04.003

[59] Lodha N, Loucks CM, Beaulieu C, et al. Congenital stationary night blindness: mutation update and clinical variability. Adv Exp Med Biol. 2012;723:371–379.

[60] Waldner DM, Bech-Hansen NT, Stell WK. Channeling vision: Ca V 1.4—A critical link in retinal signal transmission. Biomed Res Int. 2018;2018:1–14. doi: 10.1155/2018/7272630